Correlation evolution in dilute Bose-Einstein condensates after quantum quenches

J. Pietraszewicz,[1,*] M. Stobińska,[1,2,†] and P. Deuar[1,‡]
[1]*Institute of Physics, Polish Academy of Sciences, Al. Lotników 32/46, 02-668 Warsaw, Poland*
[2]*Faculty of Physics, University of Warsaw, ul. Pasteura 5, 02-093 Warsaw, Poland*

(Received 20 December 2018; published 15 February 2019)

The universal forms of quantum density and phase correlations after an interaction quench are found for dilute one-dimensional (1D), 2D, and 3D condensates. A Bogoliubov approach in a local density approximation is used. We obtain compact expressions for the most visible effects. Our results show how loss of phase coherence and antibunching are built up after the quench by quantum fluctuations. We demonstrate further that the density correlations can be observed even with imaging resolution much worse than healing length. This indicates that the direct measurement of counterpropagating atom pairs *in situ* in a continuum system is realistic. The conditions in contemporary 1D experiments are especially favorable for the correlation wave observations.

DOI: 10.1103/PhysRevA.99.023620

Quantum quenches are one of the fundamental quantum dynamical phenomena in many-body systems and cosmology [1–3]. They are generically induced by changes to the Hamiltonian that occur globally and nonadiabatically, and they become visible when the relevant energy scale rises above the thermal one. Cold atom systems have enabled the investigation of this kind of nonequilibrium quantum dynamics to an unprecedented degree. The greatest emphasis has been placed on strong quenches across a phase transition, and production of entanglement and complexity. Examples, often on lattice systems, include [4–10].

Quenches that remain within the condensate phase of dilute continuum systems are also of much interest, though less widely explored. A major motivation to understand them is that they occur in many existing experiments. Continuum quenches are interesting also because the Lieb-Robinson bound [11] does not apply to the excitations since hopping speed is not limited by a lattice. A quantum quench can be wilfully imposed by varying the tight confinement or the interaction strength. A quench can also happen as a side effect, e.g., when preparing the initial state of reduced-dimensional gases, or from a rapid loss of atoms that affects the chemical potential. Time-varying spatial correlations are induced, and indeed have been measured in contemporary cold atom experiments [5,6,12,13]

Research on quenches in dilute continuum condensates include the comprehensive work of Calabrese, Caux, and Cardy on the dynamical structure factor after a quench [14–16], the Lieb-Liniger one-dimensional (1D) model [17–20], and its long-time steady state [21]. Density correlations and waves in a 3D BEC were studied by Carusotto *et al.* [22]. The equilibration of phase correlations in 1D was measured in [12], and density structure factors have also been measured in 2D dilute gases [23,24]. Recently, an extensive study of phase coherence and momentum distributions has been made [25].

Compact analytic expressions for the quench correlations in dilute gases have not been available. It is the purpose of this paper to fill that gap. We will study a quench of the contact interaction at zero temperature, and consider uniform sections of a gas in the Bogoliubov approximation. We obtain expressions for density and phase correlations across the whole gamut of dimensionalities and postquench times. They go beyond the two earlier studies of particular cases [21,22]. This includes medium times in 1D, which we find to be especially favorable for observations with realistic detector resolution.

The resulting correlations have length scales comparable to the healing length, much shorter than the typical size of the condensate. Therefore, what we obtain can be fed into a local density approximation (LDA) to describe most nonuniform cases of interest. The first- and second-order spatial correlation functions, $g^{(1)}$ and $g^{(2)}$, give an intuitive picture of the behavior that occurs in single realizations of the gas. The shape of the correlations matches the shape of typical disturbances in the gas. Representative examples are shown in Fig. 1.

Consider a uniform d-dimensional Bose gas with contact interactions of strength g and mean density $\bar{n}$. The Hamiltonian, in terms of a Bose field $\hat{\Psi}(\mathbf{x})$, is

$$\hat{H} = \int d^d\mathbf{x}\, \hat{\Psi}^\dagger(\mathbf{x})\left[-\frac{\hbar^2}{2m}\nabla^2 + \frac{g}{2}\hat{\Psi}^\dagger(\mathbf{x})\hat{\Psi}(\mathbf{x})\right]\hat{\Psi}(\mathbf{x}). \quad (1)$$

The system has just one dimensionless parameter

$$\gamma = \left(\frac{m\,g\,\bar{n}}{\hbar^2}\right)^d \frac{1}{\bar{n}^2}. \quad (2)$$

It is identical to the Lieb-Liniger gamma parameter in the 1D gas [26], and with $\gamma = (4\pi)^3\,\bar{n}a_s^3$ in 3D, where a_s is the s-wave scattering length. In reduced dimensionalities, the confinement in the tightly bound directions affects γ, e.g., in 1D $g = 4\pi\hbar a_s \nu_\perp$, where $\nu_\perp$ is the tight trapping frequency. For our purposes, we introduce length $u_x = \hbar/mc$ and time units $t_c = mu_x^2/\hbar$, with $c = \sqrt{g\bar{n}/m}$ the speed of

*pietras@ifpan.edu.pl
†Present address: University of Warsaw.
‡deuar@ifpan.edu.pl

 ©2019 American Physical Society

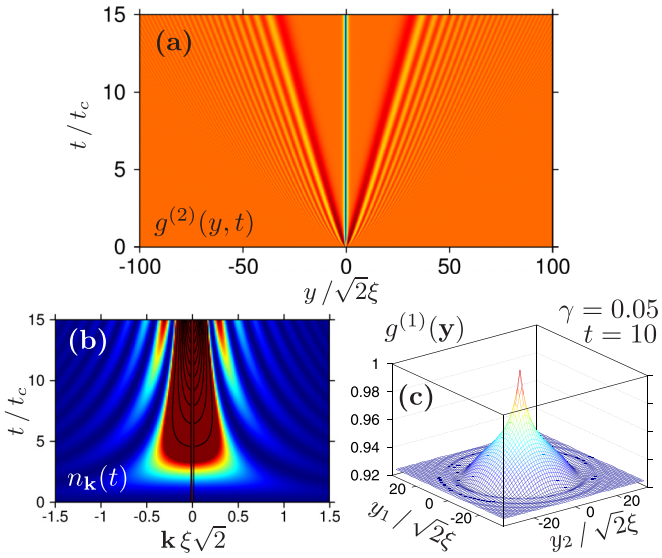

FIG. 1. Correlations after a quantum quench from $g_0 \sim 0$ to $g \gg g_0$: (a) density correlation $g^{(2)}(y,t)$ and (b) momentum distribution $n_{\mathbf{k}}(t)$ in a 1D gas, and (c) a snapshot of the phase correlation $g^{(1)}(\mathbf{y})$ in 2D. Red (blue) indicates high (low) values. The color brown in (b) is a saturated high value, with black higher contours superposed. The healing length ξ, γ parameter, distance y, and time unit $t_c = \hbar/mc^2$ are as in the text.

sound and $\xi = \hbar/\sqrt{2mg\bar{n}}$ the healing length. Setting $\hbar = m = c = 1$ one obtains dimensionless variables with $\xi = \frac{1}{\sqrt{2}}$ and $\gamma = 1/\bar{n}^2$.

Let us study the paradigmatic quench from the initially pure noninteracting condensate in the zero momentum ($\mathbf{k} = \mathbf{0}$) mode. Instantaneously at $t = 0$, the interaction is turned on to its final value $\gamma > 0$. The evolution is treated using a standard number-conserving Bogoliubov description [27], with similarities to [22]. The Bogoliubov approach boils down to two assumptions: (i) the quantum depletion $\delta N/N$, being the fraction of atoms in the noncondensate modes, is much smaller than 1, and (ii) the interaction between noncondensate modes can be neglected. Assumption (ii) is met when $\gamma \ll 1$, while (i) requires that the volume V is mostly phase-coherent. In 3D this is easily met, while in 2D and 1D it restricts the allowed box size V or time. The calculation provides values of $\delta N/N$ and $g^{(1)}(y)$ so that validity can be checked self-consistently.

To proceed, the space of volume $V = L^d$ can be discretized on an arbitrarily fine lattice with volume Δv per point $\mathbf{r}_i$. The Hamiltonian (1) then becomes

$$\widehat{H} = -J \sum_{i,j} \widehat{a}_i^\dagger \widehat{a}_j + \frac{U}{2} \sum_i \widehat{a}_i^\dagger \widehat{a}_i^\dagger \widehat{a}_i \widehat{a}_i \tag{3}$$

in terms of creation $\widehat{a}_i^\dagger$ and annihilation $\widehat{a}_i$ operators on the lattice with $J = 1/[2(\Delta v)^{2/d}]$, $U = \sqrt{\gamma}/(\Delta v)$, and mean site occupation $\Delta v/\sqrt{\gamma}$. Since a distance scale of at least the healing length is required to encompass the continuum physics, we need $\Delta v \ll 1$. This ensures that mapping of the continuum onto the lattice is sensible. On a square lattice, Δv corresponds to a maximum momentum cutoff $k_{\max} = \pi/(\Delta v)^{1/d}$, and so $J/U = \frac{1}{2\sqrt{\gamma}} (\frac{k_{\max}}{\pi})^{2-d}$.

We find the phase coherence and density correlations at a distance $y = |\mathbf{y}|$ between two points $\mathbf{r}$ and $\mathbf{r}' = \mathbf{r} + \mathbf{y}$ in terms of the dispersion relation for $k = |\mathbf{k}|$: $\omega_k = k\sqrt{1 + k^2/4}$. The normalized phase coherence is given by

$$g^{(1)}(y,t) = \frac{\langle \widehat{a}^\dagger(\mathbf{r})\widehat{a}(\mathbf{r}')\rangle}{\bar{n}\Delta v} = 1 - \frac{1}{2\bar{n}V} \sum_{\mathbf{k}\neq 0} \frac{1}{\omega_k^2} [1 - \cos 2\omega_k t - \cos \mathbf{k}\cdot\mathbf{y} + \cos(\mathbf{k}\cdot\mathbf{y} + 2\omega_k t)]. \tag{4}$$

The normalized density correlations are given by

$$g^{(2)}(y,t) = \frac{\langle \widehat{a}^\dagger(\mathbf{r})\widehat{a}^\dagger(\mathbf{r}')\widehat{a}(\mathbf{r}')\widehat{a}(\mathbf{r})\rangle}{(\bar{n}\Delta v)^2} = 1 - \frac{1}{2\bar{n}V} \sum_{\mathbf{k}\neq 0} \frac{k^2}{\omega_k^2} [\cos \mathbf{k}\cdot\mathbf{y} - \cos(\mathbf{k}\cdot\mathbf{y} + 2\omega_k t)]. \tag{5}$$

We find also the mode occupation to be

$$n_{\mathbf{k}} = [(\sin \omega_k t)/\omega_k]^2, \tag{6}$$

which appears in the quantum depletion

$$\delta N(t)/N = \frac{1}{N} \sum_{\mathbf{k}\neq 0} n_{\mathbf{k}}. \tag{7}$$

In the large system and continuum limit ($V \to \infty$, $\Delta v \to 0$) the discrete sums over $\mathbf{k}$ can be converted to integrals. Then, for each dimensionality d, one has the solutions

$$g^{(1)}(y,t) = 1 - \sqrt{\gamma} \int_0^\infty dk \left(\frac{1 - \cos 2\omega_k t}{k^2 + 4}\right) \frac{1 - M_d}{a_d\, k^{3-d}}, \tag{8}$$

$$g^{(2)}(y,t) = 1 - \sqrt{\gamma} \int_0^\infty dk \left(\frac{1 - \cos 2\omega_k t}{k^2 + 4}\right) \frac{M_d\, k^{d-1}}{a_d} \tag{9}$$

as a function of time t and distance y. The functions $M_d = M_d(k\,y)$ and constants a_d are the following:

$$M_d = \begin{cases} \cos ky & \text{for } d = 1, \\ J_0[k|y|] & \text{for } d = 2, \\ \frac{\sin ky}{ky} & \text{for } d = 3, \end{cases} \qquad a_d = \begin{cases} \pi/2 & \text{for } d = 1, \\ \pi & \text{for } d = 2, \\ \pi^2 & \text{for } d = 3, \end{cases} \tag{10}$$

and $J_\alpha[x]$ are Bessel J functions. Notably, the solutions retain the same universal shapes, and only the deviations from full coherence $g^{(\mu)} = 1$ are proportional to $\sqrt{\gamma}$. The expressions are accurate as long as the deviations are perturbative. Characteristic examples of (8) and (9) are shown in Fig. 1.

Explicit expressions for the correlations (8) and (9) can be found in various limits. Figure 1(a) depicts the two principal regimes: a timelike regime inside the sound cone, and a spacelike one outside. Between them, the main correlation wave packet is propagating at twice the speed of sound. The double speed comes about because it is composed of counterpropagating atom pairs. Representative profiles of the correlations at a given time $t = 7.5t_c$ are shown in more detail in Figs. 2 and 3.

In the *spacelike regime* $y > 2t$, at long times $t \gtrsim 1$, the density fluctuations decay to $g^{(2)}_{\text{spacelike}} = 1$. The phase

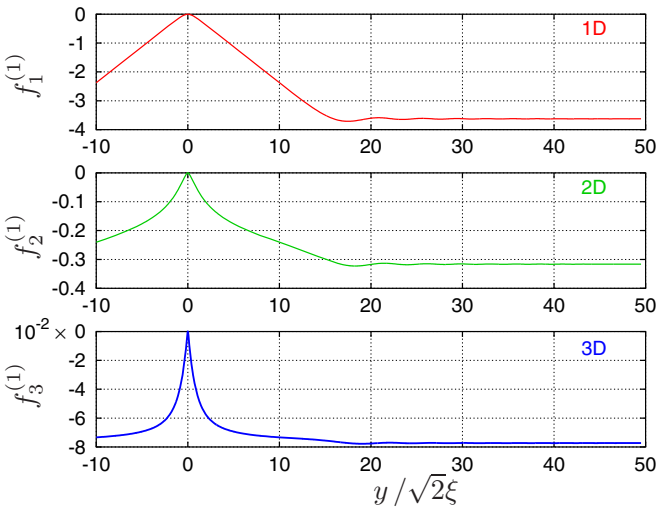

FIG. 2. Universal solutions (8) for phase coherence scaled as $f_d^{(1)} = [g^{(1)}(y,t) - 1]/\sqrt{\gamma}$, shown at long times $t = 7.5t_c$.

coherence

$$g^{(1)}_{\text{spacelike}}(y,t) \approx 1 - \delta N(t)/N \tag{11}$$

is reduced by the depletion

$$\frac{\delta N(t)}{N} \approx \sqrt{\gamma} \times \begin{cases} \frac{4t-1}{8} & \text{for } d = 1, \\ \frac{1}{4\pi}(c_1 + \ln t\,) & \text{for } d = 2, \\ \frac{1}{4\pi}(1 + c_2 e^{-c_3 t}) & \text{for } d = 3. \end{cases} \tag{12}$$

The main contributions to this reduction at long times come from phonon excitations. The constants c_j are found numerically and are $c_1 \approx 1.96(1)$, $c_2 \approx 0.43(1)$, and $c_3 \approx 2.24(2)$. We see the linear and logarithmic decay characteristic of 1D and 2D quasicondensates, respectively. Clearly, in this regime the model is breaking down at long enough times when $\delta N/N \to \approx 1$, but remains predictive for shorter ones. In the 3D case, the loss of long-range coherence stabilizes at a constant value, as expected for a BEC. However, this value

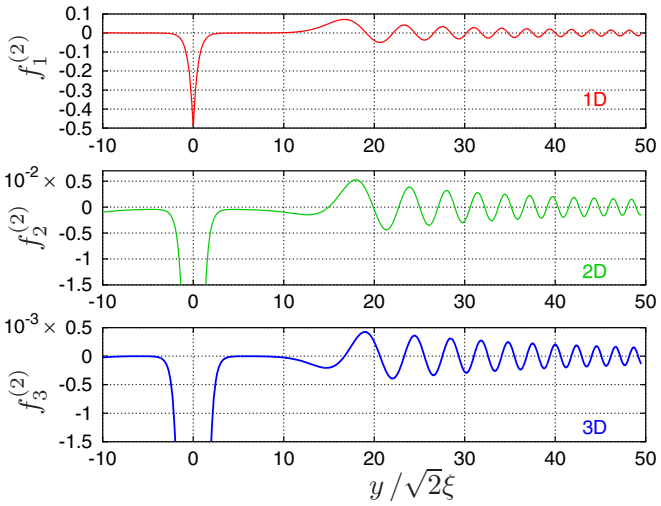

FIG. 3. Universal solutions (9) for density correlations scaled as $f_d^{(2)} = [g^{(2)}(y,t) - 1]/\sqrt{\gamma}$, shown at long times $t = 7.5t_c$.

$\delta N/N = \frac{\sqrt{\gamma}}{4\pi} \approx 0.080\sqrt{\gamma}$, seen also in [25], is larger than the ground-state value of $\frac{\sqrt{\gamma}}{3\pi^2} \approx 0.034\sqrt{\gamma}$ [28]. This indicates that the quench excites many more pairs than appear in the ground state.

In the *timelike regime* $y < 2t$, and at long times $t \gg 1$, the phase coherence,

$$g^{(1)}_{\text{timelike}}(y) \approx 1 - \sqrt{\gamma} \times \begin{cases} \frac{2y-1}{8} & \text{for } d = 1, \\ \frac{1}{4\pi}(\gamma_E + \ln y) & \text{for } d = 2, \\ \frac{1}{4\pi}\left(1 - \frac{1}{2y}\right) & \text{for } d = 3, \end{cases} \tag{13}$$

decays for $y \gtrsim 1$ to its spacelike value (11), where $\gamma_E \approx 0.5772$. The validity of the description breaks down when the deviation of $g^{(1)}$ becomes comparable with unity. This occurs for distances $y \gtrsim \frac{1}{\sqrt{\gamma}}$ in 1D and $y \gtrsim \exp(\pi/\sqrt{\gamma})$ in 2D.

The long-time density correlations

$$g^{(2)}_{\text{timelike}}(y) \approx 1 - \sqrt{\gamma} \times \begin{cases} \frac{e^{-2y}}{2} & \text{for } d = 1, \\ \frac{K_0[2y]}{\pi} & \text{for } d = 2, \\ \frac{e^{-2y}}{2\pi y} & \text{for } d = 3, \end{cases} \tag{14}$$

exhibit antibunching on a healing-length scale. $K_0[x]$ in (14) is the Bessel K function.

The state reached in (14) differs from the 1D ground state, which has antibunching of $g^{(2)}(0) = 1 - \frac{2}{\pi}\sqrt{\gamma} \approx 1 - 0.637\sqrt{\gamma}$ [29]. However, it does agree with earlier studies [21] that found the stationary state to be a peculiar one, i.e., neither thermal nor described by a generalized Gibbs ensemble. For $d \geqslant 2$, expressions (14) are divergent at $y = 0$. In practice, the dip in correlation is limited to a value determined by the accessible momentum:

$$g^{(2)}_{\text{timelike}}(0) = 1 - \sqrt{\gamma} \times \begin{cases} \frac{1}{\pi}\tan^{-1}\frac{k_{\max}}{2} & \text{for } d = 1, \\ \frac{1}{2\pi}\ln\left(1 + \frac{k_{\max}^2}{4}\right) & \text{for } d = 2, \\ \frac{1}{\pi^2}\left(k_{\max} - 2\tan^{-1}\frac{k_{\max}}{2}\right) & \text{for } d = 3. \end{cases} \tag{15}$$

The time dependence of $g^{(2)}(0)$ quantifies the onset of antibunching. It can be useful to judge prethermalization timescales. One finds that in 1D, the form

$$g^{(2)}(0) \approx 1 - \sqrt{\gamma} \times \begin{cases} \frac{3}{2}\sqrt{t} - \frac{1}{2}t^{3/2} & \text{for } t \lesssim \frac{1}{4}, \\ \frac{1}{\pi}\tan^{-1}\frac{k_{\max}}{2} - \frac{c_2 e^{-c_3 t}}{2t^{c_4}} & \text{for } t \gtrsim \frac{1}{4} \end{cases} \tag{16}$$

fits the calculated function quite well. The constants are $c_2 = 0.35(1)$, $c_3 = 2.05(1)$, and $c_4 = 0.33(2)$.

Importantly, the bulk of the timelike regime is uncorrelated because no disturbance can travel slower than the speed of sound.

On the boundary between the spacelike and timelike regimes, at $y \approx 2t$, one finds the main density correlation wave. It takes the forms

$$g^{(2)}_{\text{wave}}(y) \approx 1 + \sqrt{\gamma} \times \begin{cases} \frac{1}{2(6t)^{1/3}} F_1[-x] & \text{for } d = 1, \\ \frac{1}{2\sqrt{\pi y}(6t)^{1/2}} F_2[-x] & \text{for } d = 2, \\ \frac{1}{2\pi y(6t)^{2/3}} F_3[-x] & \text{for } d = 3, \end{cases} \tag{17}$$

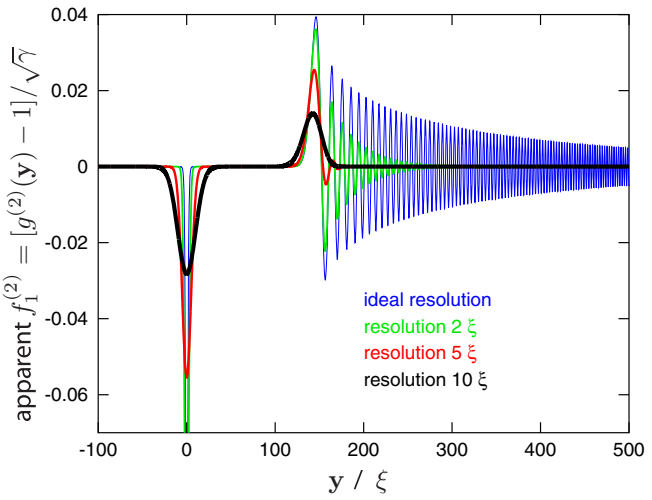

FIG. 4. Density correlations $g^{(2)}(\mathbf{y})$ at $t = 50t_c$ in 1D when seen with limited resolution. The number and amplitude of oscillations decrease as resolution worsens. From perfect (dark thin line), through 2ξ, 5ξ, to 10ξ (thick line).

where $x = (\frac{4}{3t})^{1/3}[y - 2t]$ is a scaled coordinate measuring the distance to the sound cone edge,

$$F_d[x] = \frac{1}{\pi}\int_0^\infty du\, u^{\frac{d-1}{2}} \cos\left[xu + \frac{u^3}{3} + \frac{\pi}{4}(d-1)\right] \qquad (18)$$

are generalizations of the Airy function Ai, and for instance $F_1[x] = \mathrm{Ai}[x]$. In the same boundary region as (17), the phase coherence $g^{(1)}$ has corresponding less visible oscillations. They can be seen to the right of the kink in Fig. 2, beyond the sound cone. This feature is also seen in [25], but in earlier Luttinger liquid predictions [12] it was absent.

Experiments, whether with absorption or phase-contrast imaging [30], have resolutions of many healing lengths ξ. Hence, the decay of coherence, $g^{(1)}$, inside the sound cone is directly resolvable, but not the antibunching dip or early correlation waves in $g^{(2)}$ (which must be measured *in situ*). However, the correlation wave retains its structure in the *scaled* length variable x, becoming magnified with time as $t^{1/3}$ and resolvable if the wave can survive intact for long enough. Simultaneously, its amplitude decays as $t^{-(2d-1)/3}$. In Fig. 4 we emulate imperfect resolution measurements by convolving long-time $g^{(2)}(y)$ with Gaussian point-spread functions. One sees that the primary correlation wave and the antibunching dip are robust to loss of resolution. They remain strongly visible and only mildly reduced in strength even with a (typical) resolution of $10\,\xi$. The high-velocity oscillations are rapidly lost. The remaining disturbance resembles the compact correlation wave seen with parity measurements in optical lattices [5]. Thus, finite imaging resolution leads to the appearance of an effective speed limit on what can be observed in the gas. One may see similarity to a Lieb-Robinson bound, even though one does not formally apply here.

To observe these waves in a simple manner, we should (a) have a gas that is long enough for the correlation wave to not meet the edge until it has broadened to a resolvable width, and (b) average over sufficiently many realizations for the correlation amplitude to emerge from the noise.

Let us take a look at conditions in several 1D gas experiments with ^{87}Rb. The Vienna experiment [12,30] has had $N \approx 900{-}11\,000$ atoms, trap frequencies $\nu_x \times \nu_\perp \times \nu_\perp = 7 \times 1400 \times 1400$ Hz, and observed the 1D phase correlation dynamics, similar to Fig. 2. They have an imaging resolution of 3.8 μm [31], like in more recent work [32]. The Palaiseau experiments had $N \approx 1200$ atoms, 4.5 μm resolution, trap frequencies $4 \times 3900 \times 3900$ Hz [33], or $7.5 \times 18\,800 \times 18\,800$ Hz [34].

Now, think about the correlations in the center of the cloud induced by the quench. The furthest they can cleanly propagate is a distance y of about one Thomas-Fermi radius. For the lower atom number in the Vienna experiment, the time this takes is found to be $t \approx 28t_c$ (16 ms). The rms width of the main peak rising above $g^{(2)} = 1$ is $w_{\rm rms} = 1.802 \times t^{1/3}$ and the maximum height is $h_{\rm peak} = 0.1474 \times \sqrt{\gamma}/t^{1/3}$. These give $w_{\rm rms} = 3.5$ μm, i.e., $h_{\rm peak} = 0.004$, respectively. The experimental resolution is in fact sufficient to resolve the structure even without the additional broadening seen in Fig. 4. For the correlation peak to rise out of the shot noise, the statistical uncertainty should be less than $h_{\rm peak}$. Taking a counting bin of the same size $w_{\rm rms}$ as the peak, with mean occupation $\overline{N}_{\rm bin}$, and shot noise $\mathrm{var}[N_{\rm bin}] = \overline{N}_{\rm bin}$, the variance of $g^{(2)}$ from one measurement is about $4\,\mathrm{var}[N_{\rm bin}]/\overline{N}_{\rm bin}^2$. Hence, the minimum number of realizations to average over is $4/(\overline{N}_{\rm bin}h_{\rm peak}^2) \approx 4000$. Clouds with higher atom numbers are generally less favorable both with regard to width in μm, which scales as $(N\nu_\perp v^4)^{-1/9}$, and the needed number of realizations, which scale as $(N^5 v^2/\nu_\perp^4)^{1/9}$.

The Palaiseau experiment [33] has more favorable conditions, with propagation time $t \approx 80t_c$ (28 ms), peak width $w_{\rm rms} = 3.9$ μm, max. height $h_{\rm peak} \approx 0.006$, and 2500 required realizations. A comparison with [34], which had higher $\gamma \approx 0.17$, is instructive: $t \approx 190t_c$ (15 ms), peak width $w_{\rm rms} \approx 2.5$ μm, max. height $h_{\rm peak} = 0.011$, and 1400 required realizations, i.e., better signal to noise but a narrower wave (which will be alleviated by the spreading of Fig. 4). The latest experiment [35] reports $N \simeq 4600$, $\nu_x \times \nu_\perp \times \nu_\perp = 8.8 \times 7750 \times 7750$ Hz, and resolution equal to 1.74 μm. This gives $t = 75.91t_c$ (12.78 ms), $w_{\rm rms} = 2.7$ μm, so it looks more favorable for the observation of 1D correlation waves.

Turning to the case of 2D, it is harder to observe the quench. Dips of $g^{(2)}$ seen in Fig. 3 on either side of the main peak will cancel the majority of the highest peak's contribution when resolution is poor. Moreover, the peak is lower. For example, 2D experiments in Chicago with ^{133}Cs atoms [23,36] had a resolution of 1.8 μm, and a given interaction strength $g = 0.29\frac{\hbar^2}{m}$ and temperature $T = 40$ nK. We calculate a propagation time of $t = 17.05t_c$ (11.25 ms), at which one could observe a wave width of $w_{\rm rms}^{(\rm 2D)} = 1.18\,t^{1/3} = 1.7$ μm and a wave height of $h_{\rm peak}^{(\rm 2D)} = 0.046\sqrt{\gamma}/t = 0.0007$.

In summary, we have found the universal expressions for the quantum fluctuation contribution to spatial density and phase correlations after a quantum quench in dilute Bose gases (8)–(10), displayed in Figs. 2 and 3. The medium- and long-time behavior is given as simple expressions (11)–(17) that are easily applied to assess what can be seen in a given experiment or calculation. They show how the reduction of phase coherence proceeds after a jump in interaction

strength, how antibunching accumulates, and how correlated pairs travel in the gas. The results apply mostly unchanged to cases in which a quench from g_0 to $g \gg g_0$ is made, and to temperatures for which thermal depletion is minor (generally $k_B T \lesssim g\bar{n}$). Outside of that, thermal effects or those preexisting at g_0 may be significant, while our results quantify rather the additional quantum fluctuation contribution induced by the quench. Figure 4 demonstrates that these correlations can be observed even with presently available imaging resolution. Conditions for this in 1D experiments [30,33–35] look realistic. Previously, counterpropagating atom pairs were observed with momentum measurements after expansion such as [37–40]. Looking instead at spatial correlations allows one to observe the different physics of counterpropagating atom pairs *in situ*.

We are grateful to Pasquale Calabrese, Peter Drummond, Tomasz Świsłocki, Thomas Gasenzer, Jan Zill, and Miłosz Panfil for helpful discussions. This research was supported by the Marie Curie European Reintegration Grant No. PERG06-GA-2009-256291, the Polish Government Project No. 1697/7PRUE/2010/7, and the National Science Centre (Poland) Grant No. 2012/07/E/ST2/01389.

[1] T. Langen, R. Geiger, and J. Schmiedmayer, Annu. Rev. Condens. Matter Phys. **6**, 201 (2015).
[2] F. H. L. Essler and M. Fagotti, J. Stat. Mech. (2016) 064002.
[3] A. Mitra, Annu. Rev. Condens. Matter Phys. **9**, 245 (2018).
[4] M. Kormos, M. Collura, and P. Calabrese, Phys. Rev. A **89**, 013609 (2014).
[5] M. Cheneau, P. Barmettler, D. Poletti, M. Endres, P. Schauss, T. Fukuhara, C. Gross, I. Bloch, C. Kollath, and S. Kuhr, Nature (London) **481**, 484 (2012).
[6] S. Trotzky, Y.-A. Chen, A. Flesch, I.-P. McCulloch, U. Schollwöck, J. Eisert, and I. Bloch, Nat. Phys. **8**, 325 (2012).
[7] C. Kollath, A. M. Lauchli, and E. Altman, Phys. Rev. Lett. **98**, 180601 (2007).
[8] V. Alba and P. Calabrese, SciPost Phys. **4**, 017 (2018).
[9] M. R. C. Fitzpatrick and M. P. Kennett, Phys. Rev. A **98**, 053618 (2018).
[10] U. R. Fischer, R. Schützhold, and M. Uhlmann, Phys. Rev. A **77**, 043615 (2008).
[11] E. Lieb and D. Robinson, Commun. Math. Phys. **28**, 251 (1972).
[12] T. Langen, R. Geiger, M. Kuhnert, B. Rauer, and J. Schmiedmayer, Nat. Phys. **9**, 640 (2013).
[13] C.-L. Hung, V. Gurarie, and C. Chin, Science **341**, 1213 (2013).
[14] P. Calabrese and J. Cardy, Phys. Rev. Lett. **96**, 136801 (2006).
[15] P. Calabrese and J. Cardy, J. Stat. Mech. (2007) P06008.
[16] P. Calabrese and J. Cardy, J. Stat. Mech. (2007) P10004.
[17] J.-S. Caux and P. Calabrese, Phys. Rev. A **74**, 031605(R) (2006).
[18] J.-S. Caux, P. Calabrese, and N. A. Slavnov, J. Stat. Mech. (2007) P01008.
[19] J. C. Zill, T. M. Wright, K. V. Kheruntsyan, T. Gasenzer, and M. J. Davis, Phys. Rev. A **91**, 023611 (2015).
[20] J. C. Zill, T. M. Wright, K. V. Kheruntsyan, T. Gasenzer, and M. J. Davis, New J. Phys. **18**, 045010 (2016).
[21] J. De Nardis, B. Wouters, M. Brockmann, and J.-S. Caux, Phys. Rev. A **89**, 033601 (2014).
[22] I. Carusotto, R. Balbinot, A. Fabbri, and A. Recati, EPJD **56**, 391 (2010).
[23] C.-L. Hung, X. Zhang, L.-C. Ha, S.-K. Tung, N. Gemelke, and C. Chin, New J. Phys. **13**, 075019 (2011).
[24] A. Rancon, C.-L. Hung, C. Chin, and K. Levin, Phys. Rev. A **88**, 031601(R) (2013).
[25] G. I. Martone, P.-E. Larré, A. Fabbri, and N. Pavloff, Phys. Rev. A **98**, 063617 (2018).
[26] E. H. Lieb and W. Liniger, Phys. Rev. **130**, 1605 (1963).
[27] Y. Castin and R. Dum, Phys. Rev. A **57**, 3008 (1998).
[28] F. Dalfovo, S. Giorgini, L. P. Pitaevskii, and S. Stringari, Rev. Mod. Phys. **71**, 463 (1999).
[29] K. V. Kheruntsyan, D. M. Gangardt, P. D. Drummond, and G. V. Shlyapnikov, Phys. Rev. Lett. **91**, 040403 (2003).
[30] M. Gring, M. Kuhnert, T. Langen, T. Kitagawa, B. Rauer, M. Schreitl, I. Mazets, D. Adu Smith, E. Demler, and J. Schmiedmayer, Science **337**, 1318 (2012).
[31] D. A. Smith, S. Aigner, S. Hofferberth, M. Gring, M. Andersson, S. Wildermuth, P. Krüger, S. Schneider, T. Schumm, and J. Schmiedmayer, Opt. Express **19**, 8471 (2011).
[32] S. Erne, R. Bücker, T. Gasenzer, J. Berges, and J. Schmiedmayer, Nature (London) **563**, 225 (2018).
[33] J. Armijo, T. Jacqmin, K. Kheruntsyan, and I. Bouchoule, Phys. Rev. A **83**, 021605(R) (2011).
[34] T. Jacqmin, J. Armijo, T. Berrada, K. V. Kheruntsyan, and I. Bouchoule, Phys. Rev. Lett. **106**, 230405 (2011).
[35] M. Schemmer, I. Bouchoule, B. Doyon, and J. Dubail, arXiv:1810.07170.
[36] L.-C. Ha, C.-L. Hung, X. Zhang, U. Eismann, S.-K. Tung, and C. Chin, Phys. Rev. Lett. **110**, 145302 (2013).
[37] R. R. Bücker, J. Grond, S. Manz, T. Berrada, T. Betz, C. Koller, U. Hohenester, T. Schumm, A. Perrin, and J. Schmiedmayer, Nat. Phys. **7**, 608 (2011).
[38] R. G. Dall, L. J. Byron, A. G. Truscott, G. R. Dennis, M. T. Johnsson, and J. J. Hope, Phys. Rev. A **79**, 011601(R) (2009).
[39] A. Perrin, H. Chang, V. Krachmalnicoff, M. Schellekens, D. Boiron, A. Aspect, and C. I. Westbrook, Phys. Rev. Lett. **99**, 150405 (2007).
[40] Z. Wu and H. Zhai, arXiv:1804.08251.